Proceedings of the ASME 2017 Dynamic Systems and Control Conference
DSCC 2017
October 11-13, 2017, Tysons, Virginia, USA

DSCC2017-5174

GEOMETRIC CONTROL OF QUADROTOR ATTITUDE IN WIND WITH FLOW SENSING AND THRUST CONSTRAINTS

William Craig and Derek A. Paley *
Department of Aerospace Engineering and
the Institute for Systems Research
University of Maryland
College Park, Maryland 20742
Email: wscraig@umd.edu, dpaley@umd.edu

ABSTRACT

Quadrotor vehicles show great potential over a range of tasks, but effective control in windy environments continues to be a challenge. This paper develops a thrust-saturated controller on the Lie group $SO(3)$ that uses flow sensing in order to reduce the effect of gusts on the vehicle. Designing the controller on $SO(3)$ establishes almost-global exponential stability, and avoids the pitfalls of representing rigid-body kinematics using Euler angles. We prove that exponential stability is retained in the presence of thrust saturation. Aerodynamics are incorporated into the dynamics and control through a model of the blade-flapping phenomena experienced by rotorcraft. Numerical examples show that the system control remains effective despite thrust saturation, and that flow sensing improves both the initial response and steady-state error of the system in wind.

INTRODUCTION

Quadrotor helicopters have become popular in myriad tasks, ranging from entertainment to highly utilitarian work. Their ability to hover and maneuver with great agility provides advantages over fixed-wing aircraft, and their simplicity makes them preferable over traditional helicopters.

A variety of control methods have been employed in order to stabilize quadrotors, including PID [1, 2], adaptive [3, 4], robust [5, 6], feedback linearization [7], and optimal [8] control. This paper employs a feedback linearization controller on the geometric Lie group $SO(3)$ following [7], with the addition of saturation of the vehicle's thrust inputs. Cao and Lynch [1], and Roza and Maggiore [9] approach thrust saturation using the nested saturation method from Teel [10], which is designed to address saturation in the case of a chain of integrators. Cao and Lynch [1] bound the roll and pitch angles of the system as well as the thrust by placing limits on system inputs, whereas Roza and Maggiore [9] place the bound on thrust only. Cutler and How [2] address saturation by choosing a trajectory that keeps the system states within the bounds required in order to avoid thrust saturation. This paper uses the method of Pappas et al. [11] to bound the thrust on the system in order to guarantee stability when the cost of feedback linearization does not saturate the thrust.

Quadrotors are able to accomplish an array of tasks such as surveying farmland and aiding in natural disasters [12] that require multi-rotor aircraft to fly outdoors in potentially adverse weather. High winds pose a challenge to small UAS [13–15], and developing an understanding of how they respond to wind and the mechanics behind that response is key to compensation. This paper builds on previous work [16] in order to incorporate flow sensing in the attitude controller of a three-degree-of-freedom (DOF) quadrotor test stand. In [16], the blade-flapping response of a quadrotor propeller is analyzed in order to identify the aerodynamic moment acting on a propeller in the presence of a wind gust. This moment is described analytically and may be included in the model directly, rather than using an uncertainty block characteristic of a robust-control scheme. Using traditional inertial sensing along with flow sensing to predict the aerodynamic mo-

*Address all correspondence to this author.

ment yields improved results as compared to using inertial feedback alone. Flow sensing will be performed with two-port, fore- and aft-facing probes that measure flow using differential pressure measurements [17].

Flight-dynamics applications often apply Euler angles [18] due to the intuitive nature of measuring each angle directly. However, Euler angles kinematics suffer singularities at gimbal lock and each angle is not necessarily constrained to the unit circle, which allows for non-physical error representations in the case of deviations over one rotation. We therefore use a geometric approach on the Lie group $SO(3)$, which is a compact set representing the configuration space of the orientation of a rigid body. Additionally, a geometric description of the rotational kinematics in $SO(3)$ does not encounter singularities, allowing for potentially global solutions.

The contributions of this paper are (1) the addition of propeller aerodynamics to the quadrotor dynamics, yielding a more accurate description in the presence of wind disturbances; (2) a nonlinear, feedback-linearizing controller on $SO(3)$ with saturated thrust inputs; and (3) an assessment of the relative merits of adding flow sensing to the vehicle controller versus using inertial feedback alone. We show improved stabilization through the use of flow sensing, which promises to allow for controlled flight in unfavorable weather and improved safety when flight is required in spite of weather concerns.

The outline of the paper is as follows. The first section describes the dynamics of the quadrotor vehicle. The second section describes the controller and proves stability under bounded thrust constraints. The third section shows numerical results comparing the controller with and without thrust saturation, and with and without flow sensing. The final section summarizes the paper and discusses ongoing work.

QUADROTOR DYNAMICS

This paper investigates a quadrotor constrained to operate on an attitude stand, such that the quadrotor is mounted on a ball joint at its center of mass, allowing for full attitude motion while constraining the translational degrees of freedom. Let rotation matrix $R \in SO(3)$ represent the orientation of the vehicle's body frame with respect to the inertial frame and employ rigid-body kinematics and Euler's second law to describe the rotational dynamics. We have

$$\begin{aligned} \dot{R} &= R\hat{\Omega} \\ J\dot{\Omega} &= -\Omega \times J\Omega + M_{thrust} + M_{aero}, \end{aligned} \tag{1}$$

where $\Omega = [p,q,r]^T$ is the angular velocity of the quadrotor in the body frame, M_{thrust} is the moment acting on the system due to the thrust input, M_{aero} is the aerodynamic moment on the system due to the interaction between the rotors and the wind, and J is the moment of inertia of the quadrotor. Here, J is a diagonal matrix due to the symmetry of the quadrotor; specifically $[J_1,J_2,J_3] = [m_\ell \ell^2/12 + 2m_m\ell^2, m_\ell\ell^2/12 + 2m_m\ell^2, m_\ell\ell^2/6 + 4m_m\ell^2]$ where m_ℓ is the mass of one cross-beam of the quadrotor, ℓ is the length of one cross-beam, and m_m is the mass of each motor.

The wedge operator $^\wedge$ converts a vector in $\mathbb{R}^3$ to a 3×3 skew symmetric matrix in $so(3)$, which can also be used to represent a cross product, such that for any vectors x and y in $\mathbb{R}^3$, $\hat{x}y = x \times y$. The inverse of the wedge operator is the vee operator $^\vee$, which transforms a matrix in $so(3)$ to a vector in $\mathbb{R}^3$.

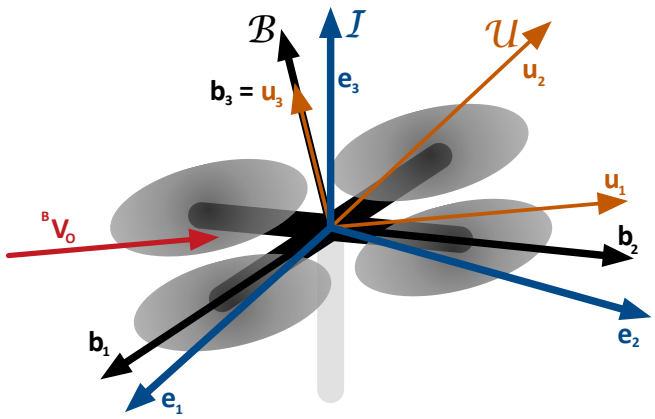

FIGURE 1. QUADROTOR ATTITUDE CONTROL TEST STAND

The quadrotor vehicle is modeled as two perpendicular uniform beams of length ℓ attached at their centers, with a rotor at both ends of each beam in a plane orthogonal to $\mathbf{b}_3$ as seen in Fig. 1. Rotors are offset from the beam plane at O by a small distance $d \ll \ell/2$ that is neglected in calculation. Define rotors 1 and 2 as those on the $\mathbf{b}_1$ axis, and rotors 3 and 4 as those on the $\mathbf{b}_2$ axis. Assume that rotors 1 and 2 spin in the positive $\mathbf{b}_3$ direction, whereas rotors 3 and 4 spin in the negative $\mathbf{b}_3$ direction, which results in a net zero torque in the $\mathbf{b}_3$ direction under nominal conditions with each rotor operating at the same speed and no outside aerodynamic forces.

While the equations of motion appear straightforward in (1), the aerodynamic moment term M_{aero} is a complicated expression due to the dynamics of each rotor in the wind field. Indeed, we introduce an additional reference frame in order to describe the aerodynamic forces, which depend on the magnitude and direction of the wind. Let $^{\mathcal{I}}\mathbf{V}_O$ represent the inertial velocity of the wind at O, and $^{\mathcal{B}}\mathbf{V}_O$ represent the velocity of the wind at O experienced by an observer in the body frame, which in this case is the same as $^{\mathcal{I}}\mathbf{V}_O$. Define the wind frame $\mathcal{U} \triangleq (O,\mathbf{u}_1,\mathbf{u}_2,\mathbf{u}_3)$, where $\mathbf{u}_3 = \mathbf{b}_3$, and $\mathbf{u}_1$ is the direction of the component of $^{\mathcal{B}}\mathbf{V}_O$ in the plane perpendicular to $\mathbf{b}_3$ [16], as seen in Fig. 1.

The ball-joint constraint at the quadrotor center of mass opposes all forces through the center of mass. All other forces and moments on the vehicle are a result of the spinning rotors. Each rotor produces a thrust, and has a corresponding torque in the direction opposite its rotation. Aerodynamic forces and moments due to non-zero external wind are taken from [16]; when a helicopter rotor moves forward in air, the advancing side of the rotor produces more lift than the retreating side, which causes a roll moment on the blades [19]. We define the azimuthal phase delay ϕ_D as the angle between the apparent maximum aerodynamic force when the advancing blade is moving directly into the wind and the maximum flapping amplitude of the blade.

The blades are set up in counter-rotating pairs, leading to cancellation of the aerodynamic moment M_{aero} along the $\mathbf{u}_1$-axis. Assume the wind components in the body frame $[{}^{\mathcal{B}}\mathbf{V}_O]_{\mathcal{B}}$ are measured by a multi-hole probe [17] and, in order to find the moment on the rotors from the resulting wind, we must identify both the phase delay ϕ_D and the magnitude β_{max} of the angle of maximum flapping. Assume that the moment due to wind on the rotors is due only to the blade spring moment k_β and the flap angle β_{max}, the rotors have negligible offset from the center of mass in the $\mathbf{b}_3$ direction (i.e., $d \approx 0$), and β_{max} is a small angle such that the thrust aligns with $\mathbf{b}_3$. We define the aerodynamic moment to be [16]

$$M_{aero} = [4k_\beta \beta_{max} S_{\phi_D} \mathbf{u}_2 \cdot \mathbf{b}_1, 4k_\beta \beta_{max} S_{\phi_D} \mathbf{u}_2 \cdot \mathbf{b}_2, 0]^T \qquad (2)$$

and the thrust moment to be

$$M_{thrust} = \left[\frac{\ell}{2}(T_3 - T_4), \frac{\ell}{2}(T_2 - T_1), c_m[(T_3 + T_4) - (T_1 + T_2)]\right]^T, \quad (3)$$

where c_m is a coefficient relating the thrust produced to the torque of the motor, found empirically.

ATTITUDE CONTROL DESIGN

By representing the kinematics using rotation matrices in the Lie group $SO(3)$, we design an attitude controller that achieves nearly global stabilization while avoiding singularities associated with Euler angles. We use the configuration error function [20]

$$\Psi(R, R_d) = \frac{1}{2}\mathrm{tr}\left(I - R_d^T R\right), \qquad (4)$$

which is locally positive definite when the angle between R and R_d, defined by $\theta_R = \arccos((Tr(R_d^T R) - 1)/2)$, is less than π [7]. The angle is less than π when $\Psi(R, R_d) < 2$, which occurs almost globally. The attitude tracking error e_R is derived from the configuration error function [7],

$$e_R = \frac{1}{2}\left(R_d^T R - R^T R_d\right)^\vee. \qquad (5)$$

The angular-velocity tracking error is [7]

$$e_\Omega = \Omega - R^T R_d \Omega_d. \qquad (6)$$

Note $d(R_d^T R)/dt = (R_d^T R)\hat{e}_\Omega$, when compared to Eqn. (1), shows e_Ω is to $R_d^T R$ as Ω is to R.

In order to minimize the rate and attitude errors, we stabilize our system using the thrust moment in Eqn. (3). The 3-DOF quadrotor attitude stand is over actuated, allowing specification of any desired configuration of three angles. In fact, in order to avoid redundant controls, three inputs are defined corresponding to the three degrees of freedom in the system:

$$\begin{aligned} \nu_1 &= T_3 - T_4 \\ \nu_2 &= T_2 - T_1 \\ \nu_3 &= (T_3 + T_4) - (T_1 + T_2). \end{aligned} \qquad (7)$$

Taking T_0 to be the nominal thrust in hover yields

$$\begin{aligned} T_1 &= T_0 - \frac{\nu_2}{2} - \frac{\nu_3}{4} \\ T_2 &= T_0 + \frac{\nu_2}{2} - \frac{\nu_3}{4} \\ T_3 &= T_0 + \frac{\nu_1}{2} + \frac{\nu_3}{4} \\ T_4 &= T_0 - \frac{\nu_1}{2} + \frac{\nu_3}{4}, \end{aligned} \qquad (8)$$

which implies

$$M_{thrust} = \left[\frac{\ell}{2}\nu_1, \frac{\ell}{2}\nu_2, c_m \nu_3\right]^T. \qquad (9)$$

Let λ_{ind} be the induced inflow ratio, and λ_{climb} be the inflow due to the motion of the vehicle, given by

$$\lambda_{climb} = 1/(\omega_j r)\left[-q\ell/2, q\ell/2, p\ell/2, -p\ell/2\right]^T. \qquad (10)$$

Following [19, pp 157], thrust T_j, $j = 1, ..., 4$ is the following function of rotor angular velocity ω_j:

$$T_j(\omega_j) = k_{T^{(1)}}\omega_j^2 - k_{T^{(2)}}(-{}^{\mathcal{B}}\mathbf{V}_O \cdot \mathbf{b}_3/(\omega_j r) + \lambda_{climb_j} + \lambda_{ind})\omega_j, \qquad (11)$$

where the thrust constants k_T are found empirically.

Applying the total moment on the system to the error dynamics yields

$$\dot{e}_R = \frac{1}{2}\left(\mathrm{tr}\left(R^T R_d\right) I - R^T R_d\right) \qquad (12)$$

and

$$\begin{aligned}\dot{e}_\Omega =& J^{-1}\left(-\Omega\times J\Omega + M_{thrust} + M_{aero}\right)\\ &+\hat{\Omega}R^T R_d\Omega_d - R^T R_d\dot{\Omega}_d.\end{aligned} \tag{13}$$

Define $H=\text{diag}\{\ell/2,\ell/2,cm\}$ and $\boldsymbol{\nu}=[\nu_1,\nu_2,\nu_3]^T$, then choose

$$\begin{aligned}\boldsymbol{\nu} = H^{-1}J\big[&-k_R e_R - k_\Omega e_\Omega - J^{-1}\left(-\Omega\times J\Omega + M_{aero}\right)\\ &-\hat{\Omega}R^T R_d\Omega_d + R^T R_d\dot{\Omega}_d\big]\end{aligned} \tag{14}$$

such that

$$\begin{aligned}M_{thrust} =& -Jk_R e_R - Jk_\Omega e_\Omega + \Omega\times J\Omega - M_{aero}\\ &+J\left(-\hat{\Omega}R^T R_d\Omega_d + R^T R_d\dot{\Omega}_d\right).\end{aligned} \tag{15}$$

When Eqn. (15) is inserted in Eqn. (13), the angular-velocity error dynamics become

$$\dot{e}_\Omega = -k_R e_R - k_\Omega e_\Omega. \tag{16}$$

Proposition 1: [7] (Exponential Stability of Attitude Dynamics) Consider the control moment M_{thrust} defined in Eqn. (15) for any positive constants $k_R,\ k_\Omega$. Suppose that the initial condition satisfies

$$\begin{aligned}&\Psi(R(0),R_d(0)) < 2\\ &||e_\Omega(0)||^2 < \frac{2}{\lambda_{min}(J)}k_R(2-\Psi(R(0),R_d(0))),\end{aligned} \tag{17}$$

where $\lambda_{min}(J)$ is the minimum eigenvalue of the inertia matrix J. Then, the zero equilibrium of the attitude tracking error $e_R,\ e_\Omega$ is exponentially stable. Furthermore, there exist constants $\alpha_2,\ \beta_2 > 0$ such that

$$\Psi(R(t),R_d(t)) \le min\{2,\alpha_2 e^{-\beta_2 t}\}. \tag{18}$$

The conditions in *Prop. 1* are satisfied almost globally, as long as $R(0)$ and $R_d(0)$ differ by less than π. Additionally, from Eqn. (17), the initial bound on the attitude rate error can be increased by increasing k_R. Considering the inherent limitations of the motors and propellers, the thrust of each propeller is saturated above by some maximum thrust T_{max} and below by zero, i.e., $0 \le T_j \le T_{max},\ j=1,...,4$.

Lemma 1: Let $T' = \min(T_{max}-T_0, T_0) > 0$. We have $T_j \le T_{max}$, for all $j=1,...,4$, provided that

$$\begin{aligned}|2\nu_2| + |\nu_3| &\le 4T'\\ |2\nu_1| + |\nu_3| &\le 4T'.\end{aligned} \tag{19}$$

Proof. Begin with the first inequality in Eqn. (19), which involves T_1 and T_2 from Eqn. (8). The second inequality follows similarly using T_3 and T_4. From (19) it can be shown that

$$\begin{aligned}-4T' \le -2\nu_2 - \nu_3 &\le 4T'\\ -4T' \le 2\nu_2 - \nu_3 &\le 4T'.\end{aligned} \tag{20}$$

Thus,

$$\begin{aligned}-T_0 \le -\frac{\nu_2}{2} - \frac{\nu_3}{4} &\le T_{max} - T_0\\ -T_0 \le \frac{\nu_2}{2} - \frac{\nu_3}{4} &\le T_{max} - T_0.\end{aligned} \tag{21}$$

Rearranging Eqn. (21) yields

$$\begin{aligned}0 \le T_0 - \frac{\nu_2}{2} - \frac{\nu_3}{4} &\le T_{max}\\ 0 \le T_0 + \frac{\nu_2}{2} - \frac{\nu_3}{4} &\le T_{max},\end{aligned} \tag{22}$$

and substituting terms from Eqn. (8) yields

$$\begin{aligned}0 \le T_1 &\le T_{max}\\ 0 \le T_2 &\le T_{max}.\end{aligned} \tag{23}$$

□

Pappas et al. [11] show that, given a feedback-linearizable system with bounded input $\dot{x} = f(x) + g(x)u, |u| \le M$, stabilizing control can be achieved if the portion of the input dedicated to feedback linearization is less than the upper bound, i.e., $|g^{-1}(x)f(x)| < M$.

In order to apply the results from [11] to our system, define $\boldsymbol{\delta} = [\delta_1,\delta_2,\delta_3]^T \triangleq H^{-1}J[-J^{-1}(-\Omega\times J\Omega + M_{aero}) - \hat{\Omega}R^T R_d\Omega_d + R^T R_d\dot{\Omega}_d]$ and $\boldsymbol{u} = [u_1,u_2,u_3]^T \triangleq H^{-1}J[-k_R e_R - k_\Omega e_\Omega]$, such that $\boldsymbol{\nu} = \boldsymbol{\delta} + \boldsymbol{u}$. We use $\boldsymbol{\delta}$ to represent the cost of feedback linearization of the error dynamics, and $\boldsymbol{u}$ to represent the stabilizing control. The following proposition represents the control authority available for stabilization by $\varepsilon > 0$.

Proposition 2: If the cost of feedback linearization $\boldsymbol{\delta}$ satisfies

$$\begin{aligned}|2\delta_2| + |\delta_3| &\le 4T' - \varepsilon\\ |2\delta_1| + |\delta_3| &\le 4T' - \varepsilon,\end{aligned} \tag{24}$$

then $\mathcal{V}(R,R_d,\Omega,\Omega_d) = 1/2 e_\Omega\cdot Je_\Omega + k_R\Psi(R,R_d) + c_2 e_R\cdot e_\Omega$, where c_2 is a positive constant, is a Lyapunov function that ensures the error dynamics of the input-constrained system Eqns. (12) and (16) are exponentially stable.

Proof. Insert $\boldsymbol{\nu} = \boldsymbol{\delta} + \boldsymbol{u}$ into Eqn. (19) to obtain

$$\begin{aligned} |2\delta_2 + 2u_2| + |\delta_3 + u_3| &\leq 4T' \\ |2\delta_1 + 2u_1| + |\delta_3 + u_3| &\leq 4T', \end{aligned} \tag{25}$$

which is satisfied if

$$\begin{aligned} |2\delta_2| + |\delta_3| + |2u_2| + |u_3| &\leq 4T' \\ |2\delta_1| + |\delta_3| + |2u_1| + |u_3| &\leq 4T'. \end{aligned} \tag{26}$$

Rewriting Eqn. (24), we find

$$\begin{aligned} |2\delta_2| + |\delta_3| + \varepsilon &\leq 4T' \\ |2\delta_1| + |\delta_3| + \varepsilon &\leq 4T'. \end{aligned} \tag{27}$$

Comparing Eqn. (27) to Eqn. (26), if we choose k_R and k_Ω such that

$$\begin{aligned} |2u_2| + |u_3| &\leq \varepsilon \\ |2u_1| + |u_3| &\leq \varepsilon, \end{aligned} \tag{28}$$

then the inputs will satisfy Eqn. (19) and, by *Lemma 1*, the thrusts will not saturate. If Eqn. (17) is also satisfied, then with positive gains k_R and k_Ω chosen to satisfy Eqn. (28), *Prop. 1* is satisfied. The zero equilibrium of the tracking error is exponentially stable [7] with $\dot{\mathcal{V}} \leq -z^T W z$, $z = [||e_R||, ||e_\Omega||]$ and

$$W = \begin{bmatrix} \frac{c_2 k_R}{\lambda_{max}(J)} & -\frac{c_2 k_\Omega}{\lambda_{min}(J)} \\ -\frac{c_2 k_\Omega}{\lambda_{min}(J)} & k_\Omega - c_2 \end{bmatrix}. \tag{29}$$

. □

PERFORMANCE EVALUATION

We now investigate conditions under which Eqn. (24) is satisfied. Consider a station-keeping scenario, such that $\Omega_d \equiv 0$, which leads to $\boldsymbol{\delta} \triangleq H^{-1}(\Omega \times J\Omega - M_{aero})$. When represented in matrix components,

$$\boldsymbol{\delta} = \begin{bmatrix} \frac{2}{\ell}[(J_2 - J_3)qr - 4k_\beta \beta_{max} S_{\phi_D} \mathbf{u}_2 \cdot \mathbf{b}_1] \\ \frac{2}{\ell}[(J_3 - J_1)pr - 4k_\beta \beta_{max} S_{\phi_D} \mathbf{u}_2 \cdot \mathbf{b}_2] \\ \frac{1}{c_m}(J_1 - J_2)pq \end{bmatrix}. \tag{30}$$

From the symmetry of the quadrotor, note $J_1 = J_2$ and $J_3 = 2J_1$, such that

$$\boldsymbol{\delta} = \begin{bmatrix} \frac{2}{\ell}[2J_1 qr - 4k_\beta \beta_{max} S_{\phi_D} \mathbf{u}_2 \cdot \mathbf{b}_1] \\ \frac{2}{\ell}[2J_1 pr - 4k_\beta \beta_{max} S_{\phi_D} \mathbf{u}_2 \cdot \mathbf{b}_2] \\ 0 \end{bmatrix}. \tag{31}$$

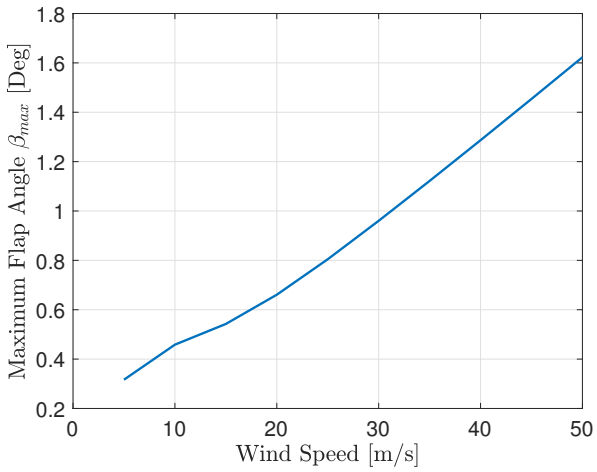

FIGURE 2. MAXIMUM FLAP ANGLE DEPENDENCY ON WIND

When applied to Eqn. (24), we have

$$\begin{aligned} \left|\frac{1}{\ell}[2J_1 pr - 4k_\beta \beta_{max} S_{\phi_D} \mathbf{u}_2 \cdot \mathbf{b}_2]\right| &\leq \left|\frac{2J_1}{\ell} pr\right| + \left|\frac{4}{\ell} k_\beta \beta_{max}\right| \leq T' - \frac{\varepsilon}{4} \\ \left|\frac{1}{\ell}[2J_1 qr - 4k_\beta \beta_{max} S_{\phi_D} \mathbf{u}_2 \cdot \mathbf{b}_1]\right| &\leq \left|\frac{2J_1}{\ell} qr\right| + \left|\frac{4}{\ell} k_\beta \beta_{max}\right| \leq T' - \frac{\varepsilon}{4}. \end{aligned} \tag{32}$$

Thus, when the system experiences zero angular velocity, we require flapping angle $\beta_{max} < \ell T'/(4k_\beta) \approx 1.1^\circ$ using the system parameters listed in Tab. 1. The equations to find β_{max} are implicit and require iteration, so we present Fig. 2 to show the relationship between flap angle β_{max} and the in-plane wind speed. Our system is expected to reach the bound on β_{max} in a 35 m/s gust. From the condition on angular velocity in Eqn. (32), when the system experiences zero wind, we require $pr < \ell T'/(2J_1)$ and $pr < \ell T'/(2J_1)$, which correspond to $pr < 50$ rad/s^2 and $qr < 50$ rad/s^2 for our parameters. Attitude bounds are satisfied when p, q, and r are each less than 7 rad/s, or alternatively, when p and q are less than 50 rad/s and r, which is not critical for station holding, is less than 1 rad/s. In practice, we can reasonably expect conditions on both wind and angular rates to be met. However, we do anticipate aerodynamic model breakdown in the case of extremely high winds as much of the retreating blade will be in reverse flow.

In order to show the effectiveness of the controller, we test it with and without saturation under the same conditions. (Note that the system model used here for testing is the full aerodynamic model from [16] rather than the simplified model used to design the controller.) Using the parameters in Tab. 1, we insert a repeated edgewise 20 m/s 1-cosine gust, shown in Fig. 3. The quadrotor's initial attitude is $R(0) = I$ and rates are $\Omega(0) = [0,0,0]^T$, with $R_d = I$ and $\Omega_d = [0,0,0]^T$. The response is shown in Fig. 4, with the corresponding control effort in Fig. 5.

TABLE 1. Model parameters

Parameter	Name	Value	Units
C_{l_α}	airfoil lift slope	2π	[ ]
λ_0	avg. inflow ratio	0.075	[ ]
ℓ	beam length	0.21	m
m_ℓ	beam mass	0.03	kg
ζ	blade damping coef.	0.026	[ ]
I_β	blade inertia	1.8×10^{-6}	kgm^2
ν_β	blade scaled nat. freq.	1.5	[ ]
θ_{tw}	blade twist	-6.6	deg
c	chord length	0.015	m
ρ	density of air	1.225	kg/m^3
e	effective hinge offset	0.1	[ ]
k_β	hinge spring const.	3	Nm/rad
γ	Lock number	1.04	[ ]
m_M	motor mass	0.018	kg
c_m	motor torque coefficient	0.0085	[ ]
N_b	number of blades	2	[ ]
T_0	propeller nom. thrust	1.3	N
Ω_p	propeller nom. ang. vel.	12,000	rpm
θ_0	root angle of attack	16	deg
m_r	rotor mass	0.0027	kg
r	rotor radius	0.0635	m
ω_{β_0}	spring nat. freq.	1290	rad/s

We also show the quadrotor response to nonzero attitude rates in Fig. 6 with no wind, $R(0) = I$, with $R_d = I$ and $\Omega_d = [0,0,0]^T$, using initial rates of $\Omega(0) = [5,5,5]^T$, with the corresponding control effort in Fig. 7. Attitude response figures use a logarithmic vertical axis to more effectively show differences in the configuration error function.

Attitude and control plots show the system with and without saturation, and with and without flow sensing. Flow sensing will be performed experimentally using custom multi-hole pressure probes that provide data through differential pressure measurements [17]. Figure 4 shows lower error in the system with flow sensing, and no difference between saturated and unsaturated thrusts. The controller is able to effectively reject the gust without saturating the thrusts, so the saturated and unsaturated systems show identical results. Figure 4 shows that the system in the presence of repeated gusts exhibits predictable deviations and returns to the equilibrium value with no destabilizing effect

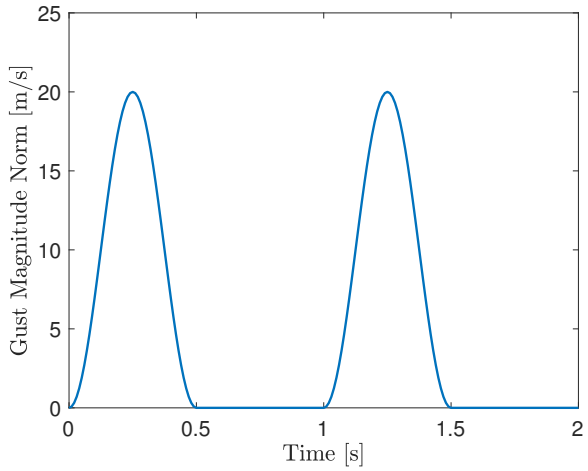

FIGURE 3. 20 M/S 1-COSINE WIND GUST PROFILE

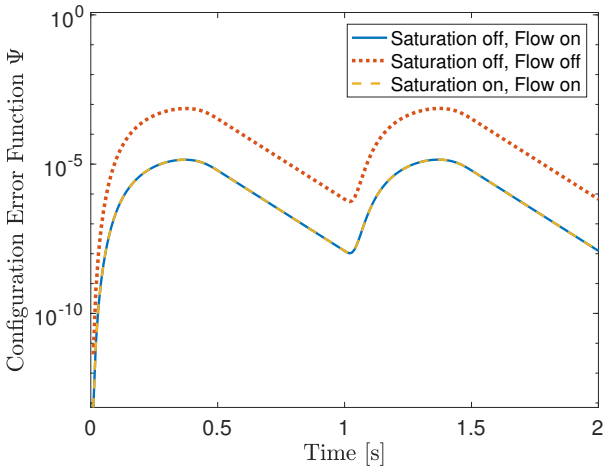

FIGURE 4. 20 M/S WIND GUST RESPONSE, $\Omega(0) = [0,0,0]^T$

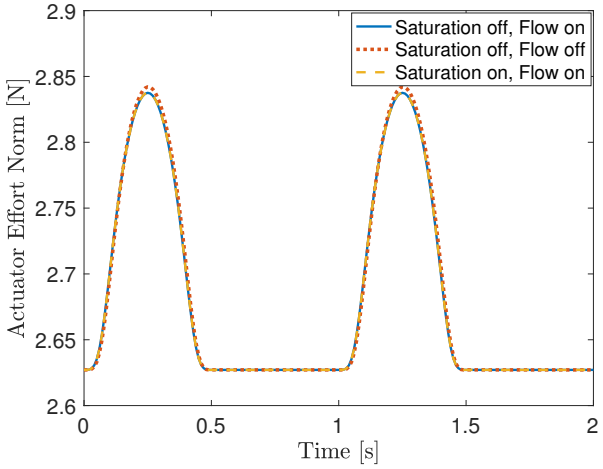

FIGURE 5. 20 M/S WIND CONTROL EFFORT, $\Omega(0) = [0,0,0]^T$

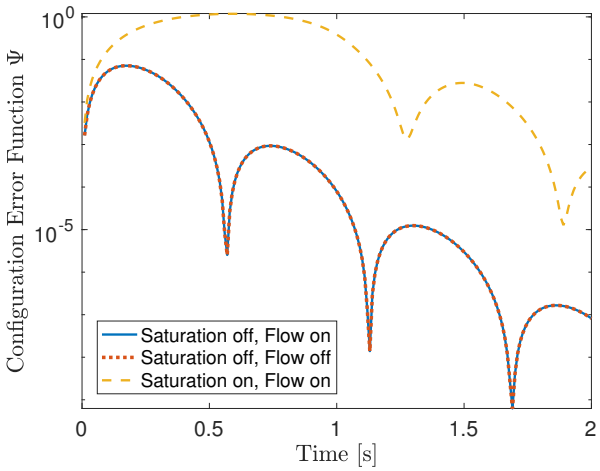

FIGURE 6. RESPONSE TO $\Omega(0) = [5,5,5]^T$, NO WIND

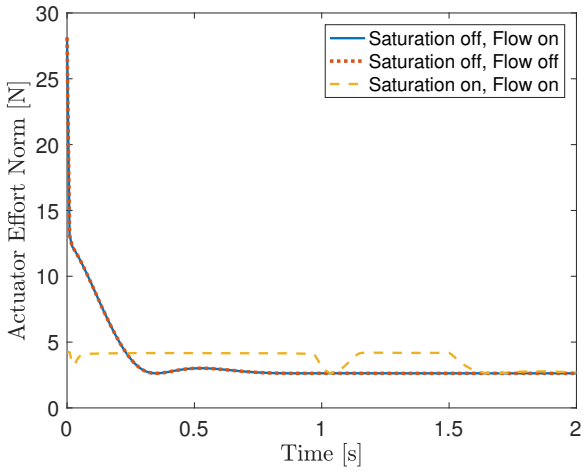

FIGURE 7. CONTROL EFFORT FOR $\Omega(0) = [5,5,5]^T$, NO WIND

due to repetition. The value of the configuration error function is very low with and without flow sensing, and when converted using the angle from the Euler axis, corresponds to approximately 0.3 degree error in the case with flow sensing versus 2 degree error in the case without flow sensing. While both attitude errors are small, we anticipate greater gains when applying the control scheme to a free-flight vehicle, where small deviations in attitude lead to increasing deviations in position. Figure 5 shows very similar control efforts between different conditions, changing only based on flow sensing. Without flow sensing the actuators respond marginally later and with slightly higher magnitude; a small change in actuation that causes nearly an order of magnitude difference in peak angular error. While the steady state error can be mitigated with an integrator in the controller, both systems will experience a similar initial error, thus the controller with flow sensing will continue to show improved performance.

In Fig. 6, nonzero initial rates cause initial deviation, then gradual return to equilibrium. In the cases without thrust saturation, the result is identical due to the absence of external flow over the vehicle, and the system quickly settles to a very low error. The rapid settling is due to an initial actuator response over five times greater than what is physically realizable, shown in Fig. 7. In the case with saturation, although the cost to feedback linearize the system does not saturate the inputs, the controller is unable to achieve the same control authority as the unsaturated cases. Input saturation effectively reduces the gains and results in larger initial deviations and a longer settling time, but nonetheless returns the system to equilibrium, showing that we can expect successful stabilization for the physical system under actuator limitations.

CONCLUSION

This paper develops the dynamics for a quadrotor vehicle on the group $SO(3)$ and includes the moment on the propellers due to aerodynamics from wind gusts. We prove exponential stability of the equilibrium point defined by desired attitude and rate in the presence of thrust saturation. Simulation studies are carried out to show the system performance, comparing cases with and without flow sensing. An experimental testbed has been developed in order to verify our controller on a physical system. In ongoing work, tests will compare performance with and without flow sensing, and will corroborate the bounds placed on our controller due to thrust saturation. As this work continues, we plan to implement our controller on a full 6-DOF system. We anticipate that station-holding and other tasks will show stability improvements through the use of flow feedback.

ACKNOWLEDGMENT

This work was supported by the University of Maryland Vertical Lift Rotorcraft Center of Excellence Army Grant No. W911W61120012.

REFERENCES

[1] Cao, N., and Lynch, A. F., 2016. "Inner-outer loop control for quadrotor UAVs with input and state constraints". *IEEE Transactions on Control Systems Technology,* ***24***(5), pp. 1797–1804.

[2] Cutler, M., and How, J. P., 2012. "Actuator constrained trajectory generation and control for variable-pitch quadrotors". In AIAA Guidance, Navigation, and Control Conf., Minneapolis, MN, pp. 1–15.

[3] Dydek, Z. T., Annaswamy, A. M., and Lavretsky, E., 2013. "Adaptive control of quadrotor UAVs: A design trade study

with flight evaluations". *IEEE Transactions on Control Systems Technology,* ***21***(4), pp. 1400–1406.

[4] Goodarzi, F., Lee, D., and Lee, T., 2015. "Geometric adaptive tracking control of a quadrotor unmanned aerial vehicle on SE(3) for agile maneuvers". *Journal of Dynamic Systems, Measurement, and Control,* ***137***(9), pp. 1–12.

[5] Kun, D. W., and Hwang, I., 2015. "Linear matrix inequality-based nonlinear adaptive robust control of quadrotor". *Journal of Guidance, Control, and Dynamics,* ***39***(5), pp. 1–13.

[6] Lee, T., Leok, M., and Mcclamroch, N. H., 2013. "Nonlinear robust tracking control of a quadrotor UAV on SE(3)". *Asian Journal of Control,* ***15***(2), pp. 391–408.

[7] Lee, T., Leok, M., and Mcclamroch, N. H., 2010. "Geometric tracking control of a quadrotor UAV on SE(3)". In IEEE Conf. on Decision and Control, Atlanta, GA, pp. 5420–5425.

[8] Alexis, K., Nikolakopoulos, G., and Tzes, A., 2010. "Constrained-control of a quadrotor helicopter for trajectory tracking under wind-gust disturbances". In IEEE Mediterranean Electrotechnical Conf., Valletta, Malta, pp. 1411–1416.

[9] Roza, A., and Maggiore, M., 2014. "A class of position controllers for underactuated VTOL vehicles". *IEEE Transactions on Automatic Control,* ***59***(9), pp. 2580–2585.

[10] Teel, A. R., 1992. "Global stabilization and restricted tracking for multiple integrators with bounded controls". *Systems and Control Letters,* ***18***(3), pp. 165–171.

[11] Pappas, G., Lygeros, J., and Godbole, D., 1995. "Stabilization and tracking of feedback linearizable systems under input constraints". In IEEE Conf. on Decision and Control, New Orleans, LA, pp. 1–34.

[12] Rabbath, C., and Lechevin, N., 2010. *Safety and Reliability in Cooperating Unmanned Aerial Systems*. World Scientific Publishing Co., Singapore, Chapter 1.

[13] Atkins, E. M., 2010. "Risk identification and management for safe UAS operation". In Int. Symp. on Systems and Control in Aeronautics and Astronautics, Harbin, China, pp. 774–779.

[14] Zarovy, S., Costello, M., and Mehta, A., 2012. "Experimental method for studying gust effects on micro rotorcraft". *Journal of Aerospace Engineering,* ***227***(4), pp. 703–713.

[15] Lu, H., Liu, C., Guo, L., and Chen, W.-H., 2015. "Flight control design for small-scale helicopter using disturbance-observer-based backstepping". *Journal of Guidance, Control, and Dynamics,* ***38***(11), pp. 2235–2240.

[16] Craig, W., Yeo, D., and Paley, D. A., 2016. "Dynamics of a rotor-pendulum with a small, stiff propeller in wind". In ASME Dynamic Systems and Controls Conf., Minneapolis, MN, pp. 1–10.

[17] Yeo, D., Sydney, N., and Paley, D., 2015. "Onboard flow sensing for downwash detection and avoidance on small quadrotor helicopters". In AIAA SciTech, pp. 1–12.

[18] Etkin, B., 1982. *Dynamics of Flight: Stability and Control*, 2nd ed. Wiley, New York, NY.

[19] Leishman, J. G., 2006. *Principles of Helicopter Aerodynamics*, 2nd ed. Cambridge University Press, New York, NY, Chapter 2,3,4.

[20] Bullo, F., and Lewis, A. D., 2005. *Geometric Control of Mechanical Systems*. Springer, New York, NY.